Geocarto International

ISSN: 1010-6049 (Print) 1752-0762 (Online) Journal homepage: http://www.tandfonline.com/loi/tgei20

# Using cosmo-skymed images to detect wet snow cover on the Kraków Ice Field, King George Island, Antarctica

Kátia Kellem da Rosa, Cláudio Wilson Mendes Jr., Jorge Arigony-Neto & Jefferson Cardia Simões

**To cite this article:** Kátia Kellem da Rosa, Cláudio Wilson Mendes Jr., Jorge Arigony-Neto & Jefferson Cardia Simões (2015): Using cosmo-skymed images to detect wet snow cover on the Kraków Ice Field, King George Island, Antarctica, Geocarto International, DOI: 10.1080/10106049.2015.1110206

**To link to this article:** http://dx.doi.org/10.1080/10106049.2015.1110206

Published online: 02 Dec 2015.

GEOCARTO INTERNATIONAL, 2015
http://dx.doi.org/10.1080/10106049.2015.1110206

Taylor & Francis
Taylor & Francis Group

# Using cosmo-skymed images to detect wet snow cover on the Kraków Ice Field, King George Island, Antarctica

Kátia Kellemda Rosa[a], Cláudio Wilson Mendes Jr.[a,b], Jorge Arigony-Neto[b] and Jefferson Cardia Simões[a]

[a]Centro Polar e Climático, Pós-Graduação em Geografia e Pós Graduação em Sensoriamento Remoto, Instituto de Geociências, Universidade Federal do Rio Grande do Sul, Porto Alegre, Brazil; [b]Laboratório de Monitoramento da Criosfera, Universidade Federal do Rio Grande, Rio Grande, Brazil



**ABSTRACT**

This work analysed the spatio-temporal variation of snow cover on the Kraków Ice Field, located in the King George Island, Antarctica. High spatial resolution images of COSMO-SkyMed were used in this study. These X-band images are vertically and horizontally co-polarized and their intensity data were converted to amplitude (dB). The COSMO-SkyMed images were classified by a minimum distance algorithm and post-classified based on knowledge of adjacency relationships of snow zones. Hypsometric, slope, aspect and solar radiation maps to support the interpretation of backscatter patterns in the COSMO-SkyMed images. Three radar zones were classified in these images: percolation, slush and wet snow radar zone. Positive surface air temperatures and rainfall events, registered from a meteorological station, lead to increase in wet snow and slush zones. The COSMO-SkyMed images and minimum distance algorithm were adequate to discriminate the snow cover and to assess the supraglacial melting pattern during the ablation season in the study area.

**ARTICLE HISTORY**
Received 9 July 2015
Accepted 5 October 2015

**KEYWORDS**
Polar remote sensing; snow wet zone; radar imagery

## Introduction

Glaciers are masses of snow and ice that may have superficial facies or zones, according to their surface and stratigraphic characteristics, such as areas of dry snow, percolation, wet snow and bare ice zones, forming an ordered sequence from Ice Field interior to ice front. In the dry snow zone, there is no surface melting even in the summer and it is only found in the interior of ice sheets and in high mountains. The percolation zones have surface melting, but the water percolates few metres and refreezes, forming ice lenses or glands, while in the wet snow zone, the snowpack is saturated with water. The bare ice zone occurs in the glacier ablation area and it has an irregular surface of exposed glacier ice (Cuffey & Paterson 2010).

Several studies developed methods for mapping global snow cover using optical data. Hall, Foster et al. (1995), Hall, Riggs et al. (1995), Partington (1998), and Hall et al. (2002, 2010, 2015) calculated the snow-extent variability using Landsat TM (Thematic Mapper) and ETM+ (Enhanced Thematic Mapper Plus) and Terra MODIS (Moderate Resolution Imaging Spectroradiometer). Synthetic Aperture Radar

**CONTACT** Kátia Kellem da Rosa katia.rosa@ufrgs.br

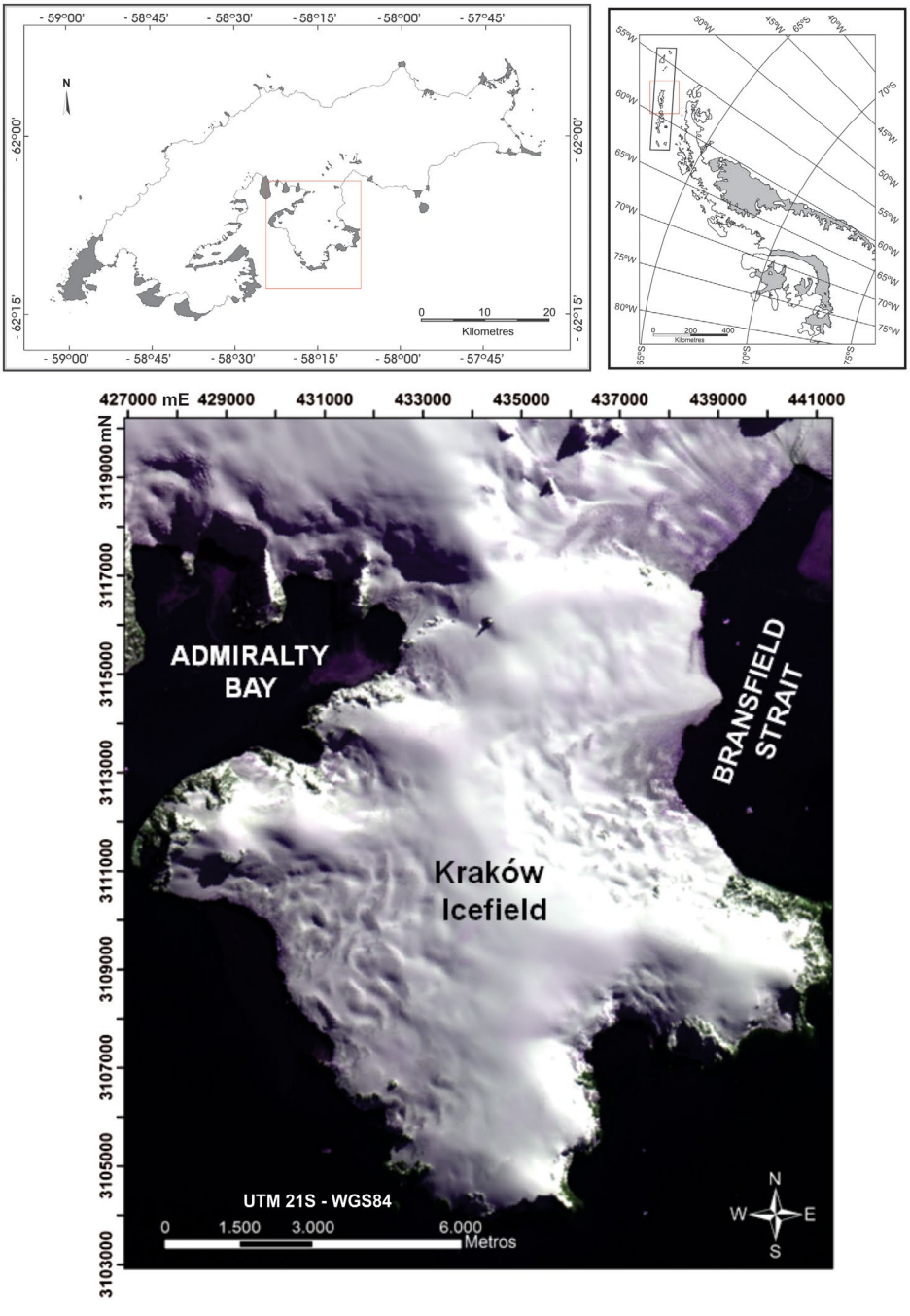


**Figure 1.** Location of the Kraków Ice Field in the King George Island, Antarctica. The red square indicates the ground swath area of the COSMO-SkyMed scenes used in this study.

(SAR) data have also used for snow-covered detection. RADARSAT, ERS and ENVISAT Advanced Synthetic Aperture Radar (ASAR) images (C-band – 5.6 GHz) were used for the identification of radar zones in glaciers (Forster et al. 1996; Braun & Rau 2000; Rau et al. 2000; König et al. 2001; Rao 2002; Arigony-Neto 2006; Jensen 2007; Mendes 2011). The sensitivity of the radar signal to the snow-covered properties, such as the presence of liquid water, makes it a highly valuable tool to study snow-covered dynamics in remote areas, as demonstrated by Braun and Rau (2000) and Rau et al. (2000).

The formation of the radar zones is determined by metamorphic processes within the snowpack, driven by the meteorological conditions prior to and during image acquisition. Consequently, these radar zones are dynamic on a time scale of days to weeks and exhibit remarkable inter-annual variations (Rau et al. 2001). These changes represent the responses of the energy balance and are considered to be a proxy of climatological variability, providing information regarding the occurrence of singular high-temperature events affecting the uppermost areas of the glacial systems (Rau et al. 2000).

According to Liu et al. (2005), measuring the spatial extent of different snow zones and monitoring the variations in the geographical position of the snow zone boundaries are important to the understanding of regional climatic fluctuation and the hydrological responses of stream systems. These snow zones can be detected and monitored by SAR sensors. The microwave radiation emitted by these active sensors is able to penetrate through clouds and most rain (CCRS 2002). Variations of the backscatter values in radar images are the results of changes in the physical characteristics of terrain surfaces illuminated by the radar beam, such as material sediment, moisture content, surface roughness and its geometry (e.g. local incidence angle), as cited by Sarapirome et al. (1995). The side-looking viewing geometry of imaging radar systems improves the recognition of glacial surface zones.

The advent of high-resolution X-band SAR images, like COSMO-SkyMed, allows to detect more feature details and can be used to support glacial studies (ASI 2007; Battazza et al. 2007; Caltagirone et al. 2007; Coletta et al. 2008; Covello et al. 2008; Rosa et al. 2013; Andrade et al. 2015).

This study aims to investigate the spatio-temporal variability of the wet snow, percolation and slush (soaked) zones on the Kraków Ice Field, located in the King George Island (KGI), north-western tip of the Antarctic Peninsula (Figure 1), using four COSMO-SkyMed images of different dates.

The Kraków Ice Field has tidewater glaciers with steep slopes, high ice flow velocities and extensive crevasse fields, and some of the glaciers have termini on land, such as Wanda, Dragon and Professor. The equilibrium line altitude in KGI occurs between 300 and 350 m (Simões et al. 2004)). According to Braun and Rau (2000), the firn line elevations ranged between 160 and 270 m on KGI.

The maritime sub-polar climate in the South Shetland Islands is often affected by storms generated in the Pacific Ocean, which results in high rates of local precipitation. The mean summer air temperature can reach 2.8 °C, which results in high melt-water production during the summer months (Simões et al. 2004).

Ice temperature measurements have indicated that ice masses in the accumulation areas of KGI are near to pressure melting points (Macheret et al. 1997; Simões et al. 2004; Travassos & Simões 2004). Ground Penetrating Radar (GPR) reflections determined the internal structure with supraglacial, englacial and subglacial meltwater drainage in the summer (2011) and evidenced a temperate ice in the Wanda Glacier ablation area (Rosa, Fernandez et al. 2014).

Several studies have provided evidence of glacier retreat in the KGI since the mid-twentieth century (Simões & Bremer 1995; Bremer 1998; Park et al. 1998; Simões et al. 2004; Braun & Gossmann 2002). The Wanda, Viéville, Dragon and Krak glaciers, located in Kraków Ice Field, are small drainage basins and show higher retreat rates through supraglacial fusion processes if compared to other glaciers in KGI (Rosa, Freiberger et al. 2014, Rosa et al. 2015). Due to their thermal conditions, small sizes and a high retreat rate Kraków glaciers can be respond rapidly to climatic variations and are relevant for environmental studies (Rosa, Freiberger et al., 2014, Rosa et al. 2015).

The retreat of this glacier may be related to the atmospheric warming recorded over the last 60 years (Blindow et al. 2010). Over the past 30 years, the number of days with liquid precipitation has increased in the summer, thereby accelerating the snowmelt of local glaciers (Ferrando et al. 2009; Rosa, Fernandez et al. 2014)).

## Dataset

We used two horizontal-polarized (HH) and two vertical-polarized (VV) images of COSMO-SkyMed. This satellite/sensor is the largest Italian investment in space systems for Earth observation and was commissioned and funded by the Italian Space Agency (ASI). The COSMO-SkyMed

**Table 1.** Characteristics of COSMO-SkyMed images used in this study.

| Acquisition date | Acquisition time (UTC) | Satellite mission | Orbit number | Look angles near – far range | Polarization mode |
|---|---|---|---|---|---|
| 22 January 2011 | 19 h 58 min 45 s | CSK3 | 12,142 | 43.023 – 43.431 | VV |
| 25 January 2011 | 20 h 22 min 40 s | CKS1 | 19,904 | 28.329 – 28.992 | HH |
| 10 February 2011 | 20 h 22 min 30 s | CSK1 | 19,667 | 28.295 – 28.958 | VV |
| 11 February 2011 | 19 h 52 min 34 s | CSK2 | 17,193 | 45.553 – 45.916 | HH |

mission consists of a constellation of four low Earth orbit mid-sized satellites, each equipped with a multi-mode high-resolution SAR operating at the X-band (9.6 GHz), acquiring images every 12 h for a 600-km swath width. These satellites allow full global coverage and have an all-weather, day/night acquisition capability, fast revisit/response time and interferometric/polarimetric capability. The images used in this study were acquired during our fieldwork, carried out in January and February, 2011, in descending orbits and in spotlight mode, with ground resolution of 1 m, covering approximately 100 km² of ground swath. Other characteristics of COSMO-SkyMed images are described in Table 1.

The high-resolution DEM of the study area were generated by vertical aerial photographs at a scale of 1:50,000, acquired on January 2003 by the Servicio Hidrográfico y Oceanográfico de La Armada de Chile (SHOA). Control points in the Kraków Ice Field were surveyed in the summers of 2007, 2010 and 2011, by Differential Global Positioning System (DGPS), using a topographic receiver (model GTRA). Besides that photographic records and a GPR survey were carried out by Rosa, Fernandez et al. (2014) in January and February 2011, during the COSMO-SkyMed image acquisitions.

Daily mean air temperature and liquid precipitation records were obtained from the Eduardo Frei Montalva Station (62°05′S, 58°23.5′W), a meteorological station managed by the Dirección Meteorológica de Chile – Dirección General de Aeronáutica Civil, located at Fildes Peninsula, KGI.

## Methodology

### *Image processing*

The COSMO-SkyMed level 1A products (also indicated as Single-look Complex Slant – SCS) were used in this work. These products are focused data, with internal radiometric calibration, in slant range-geometric projection, with associated ancillary data. Data processing chain comprises the conversion from intensity to amplitude values (dB), speckle filtering and geometric corrections. It was performed using the open source software Next ESA SAR Toolbox (NEST – Array Systems Computing, Inc.).

A median filter (Rees & Satchell 1997) with a 5 × 5 kernel size was applied for speckle reduction of the COSMO-SkyMed calibrated images. This filter effectively reduced the speckle noise, preserved the edges between homogeneous areas and allowed good identification of the glacial surface characteristics. An experimental study performed by Arigony-Neto (2006) with ERS SAR and ENVISAT ASAR images indicated that the median filter is one of the best algorithms for speckle reduction in glacial environments, with high computational efficiency.

The slant-to-ground range correction was performed using image metadata and a DEM with a ground resolution of 0.7 m. This high-resolution DEM and an orthophotomosaic were generated in a digital photogrammetric station (Leica Photogrammetry Suite – Leica Geosystems, Inc.). The control points used in the external orientation of these photographs were surveyed by DGPS in the summers of 2007, 2010 and 2011. In the orthorectification of the COSMO-SkyMed images and SHOA aerial photographs, the original pixel size was resampled to a ground resolution of 0.7 and 1 m, respectively, using a bilinear interpolation. These data were represented in UTM projection and referenced to the WGS84 ellipsoid. The planimetric root-mean-square error (RMSE) of our DEM and COSMO-SkyMed images was 0.84 m and 1.2 m, respectively, which was considered satisfactory for the spatio-temporal analysis of snow cover and supraglacial melting on the Kraków Ice Field.

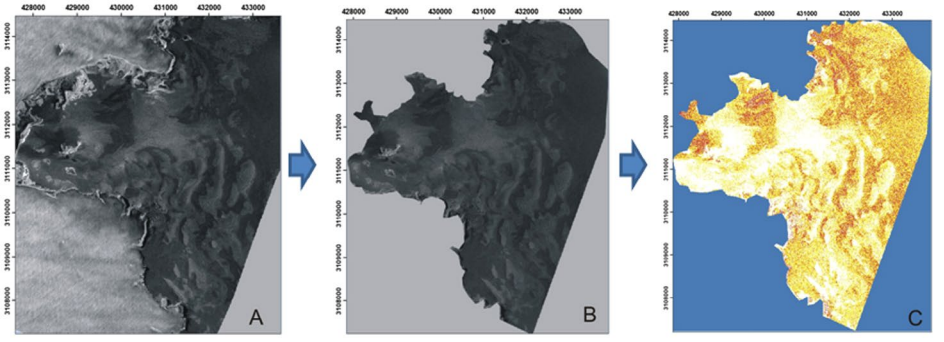


**Figure 2.** (A) Conversion from intensity to amplitude (dB), speckle filtering and orthorectification. (B) The COSMO-SkyMed images were masked by a polygon digitized of the Kraków Ice Field catchment area. (C) Image classification by Euclidean distance algorithm and image post-processing by morphological filter.



### *Image classification*

We digitized the limits of the Kraków Ice Field catchment area and used them to mask the COSMO-SkyMed orthorectified images. These clipped images were used to detect the wet snow and percolation radar zones on the study area, by a minimum distance classifier, where each pixel was classified based on its Euclidean distance from the classes' means derived from training sites collected in these images.

Visual interpretation of COSMO-SkyMed images was supported by fieldwork carried out in January and February 2011, during the same period of image acquisition. Training samples were collected in transects, as represented in Figure 6(b). All of these samples were photographed and surveyed in different glacial surface sites and their location was determined by DGPS survey. These data were used in a GIS/remote sensing environment. Fieldwork data collection was planning according to the presence of different targets (snow, slush and percolation zones, progressing from high to slow areas, respectively) that indicated glacier surface changes during the images acquisition.

In this study, we used the backscattering and elevation thresholds of the percolation and the wet snow radar zones determined by Rau et al. (2000) to classify these glacier zones in COSMO-SkyMed images. The classified pixels were grouped into contiguous classes by clump analysis, and we eliminated clumps smaller than 3 pixels using a morphological filter (Opening and Closing) to generate more continuous radar glacier zones (Figure 2).

The high-resolution DEM generated in this study was used in ArcGIS environment to derive hypsometric, slope, aspect, horizontal and vertical curvature and solar radiation maps, which were compared with the COSMO-SkyMed backscattering patterns and the radar zones classified in these images.

We examined the relationship between our mapped wet snow cover and melting dynamics and daily mean superficial air temperature and liquid precipitation data in January and February 2011, recorded by the Eduardo Frei Montalva Station (62°05′S, 58°23.5′W).

## Results

The percolation, slush and wet snow radar zones classified in the COSMO-SkyMed images are show in Figure 3. We evaluated the accuracy of these classified images by 240 samples randomly distributed in the study area, and the minimum Kappa index was 0.81, which indicates very good strength of agreement with ground truth. In the COSMO-SkyMed images at the X-band, we could easily discriminate two categories of wet snow radar zones from the percolation radar zone because they exhibited the lowest backscattering values: these zones can also be observed in the statistical data (Table 2) calculated from the training sites used in the supervised classification, described in the methodology section.

The vertically and horizontally co-polarized images were suitable to discriminate the wet snow zone from the percolation radar zone of the study area. The high spatial and radiometric resolution

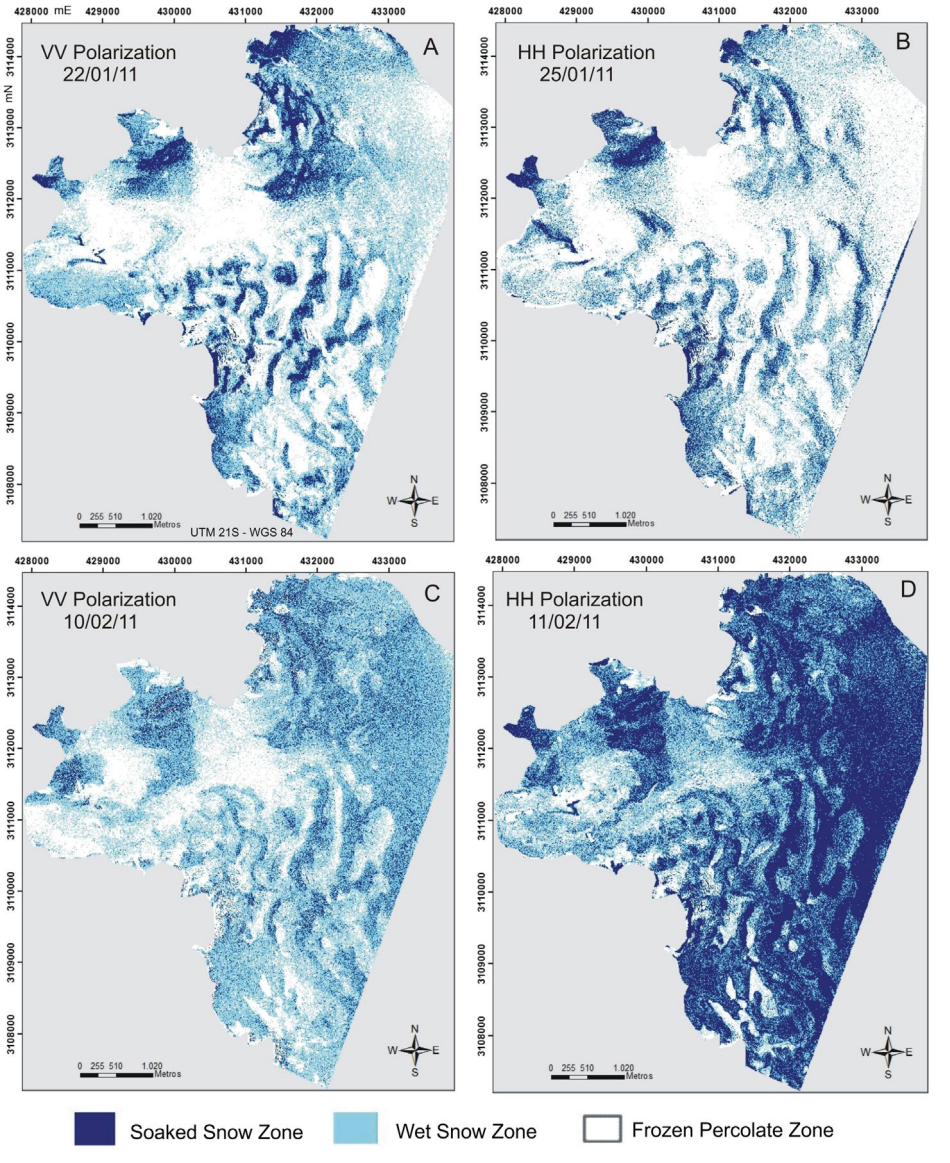


**Figure 3.** Radar glacier zones on the Kraków Ice field at different acquisition dates, classified using COSMO-SkyMed imagery at (A) VV polarization (22 January 2011); (B) HH polarization (25 January 2011); (C) VV polarization (10 February 2011); (D) HH polarization (11 February 2011). The most extensive melting area (slush and wet snow radar zones) was observed on February 11, when the liquid water in the snow pack absorbed most of the radar signal.

**Table 2.** Backscattering (dB) of the frozen percolation, wet snow and soaked snow radar zones in the Kraków Ice Field, in the COSMO-SkyMed images using VV polarization (22 January 2011).

| Class (dB) | Minimum | Maximum | Mean | Std. Dev. |
|---|---|---|---|---|
| Frozen percolation zone | −20.058 | −4.767 | −11.577 | 1.821 |
| Wet snow zone | −25.329 | −8.702 | −15.702 | 1.711 |
| Soaked snow zone | −24.730 | −11.374 | −18.443 | 1.691 |

of the COSMO-SkyMed images acquired using the spotlight mode allowed the distinction of subtle transitions of the backscattering between these radar zones, including the differences within the wet snow radar zone, such as the slush snow areas mapped in this study.

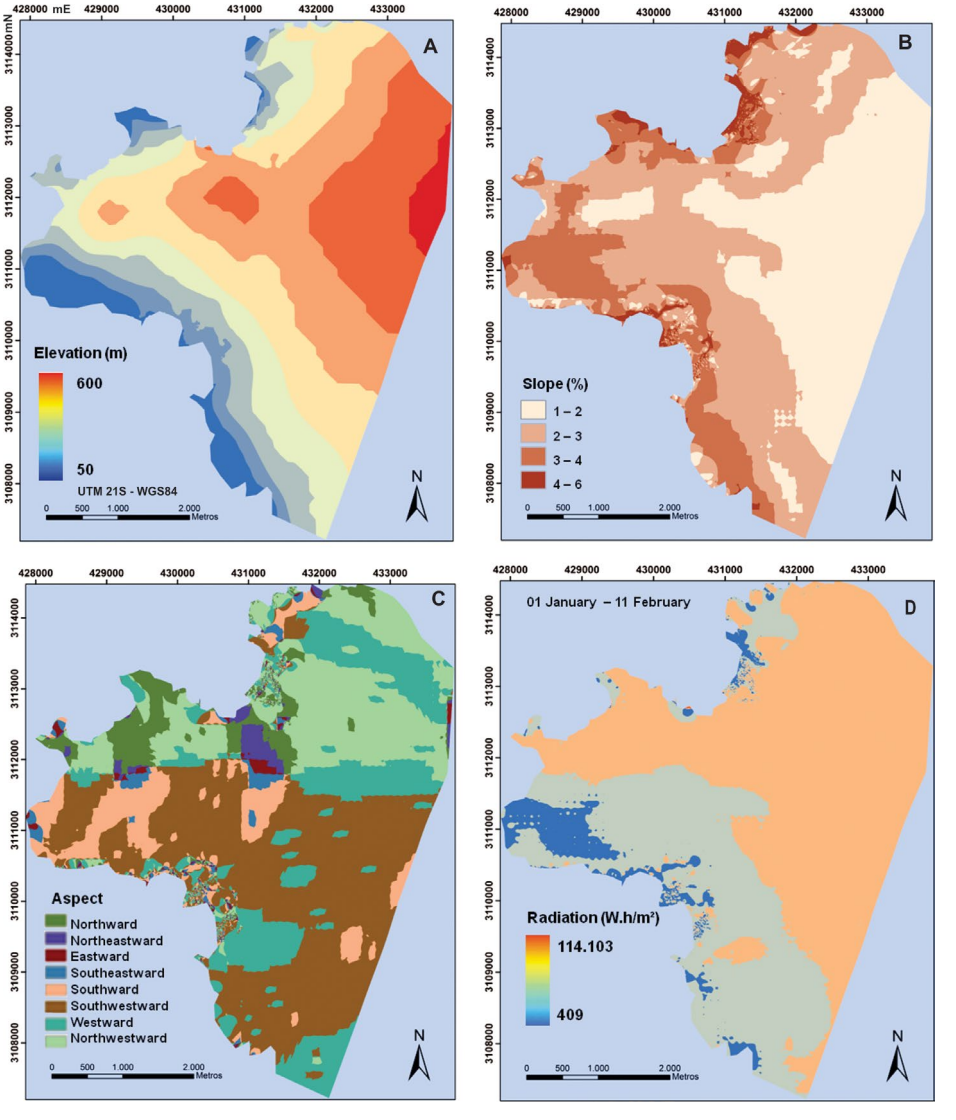


**Figure 4.** Hypsometric (A), slope (B), aspect (C) and solar radiation (D) maps derived from the high-resolution DEM generated in this study.

## Discussion

The most extensive melting areas observed in COSMO-SkyMed images occurred on February 11, when the liquid water in the snow pack absorbed most of the radar signal (Figure 3(D)). Frequent or occasional melt-freeze-cycles led to the formation of a percolation radar zone. The percolation zone was more persistent in all images analysed, in the highest and southward areas, with a low solar radiation incidence in the Kraków Ice Field (Figures 3(A)–(D) and 4(A)–(D)). However, there were percolation zones near the lowest areas of the Wanda and Dragon glaciers, with both glaciers having a terminus in Admiralty Bay and have thinning of the frontal ice mass (1–3 m). The highest areas of the Kraków Ice Field close to the Admiralty Bay exhibited more percolation zones than the areas near the Bransfield Strait (Figures 1 and 4(A)).

The wet snow radar zones have a smooth texture and dark appearance (i.e. low backscattering). According to Rau et al. (2000), the penetration depth in the wet snow radar zones is reduced to only

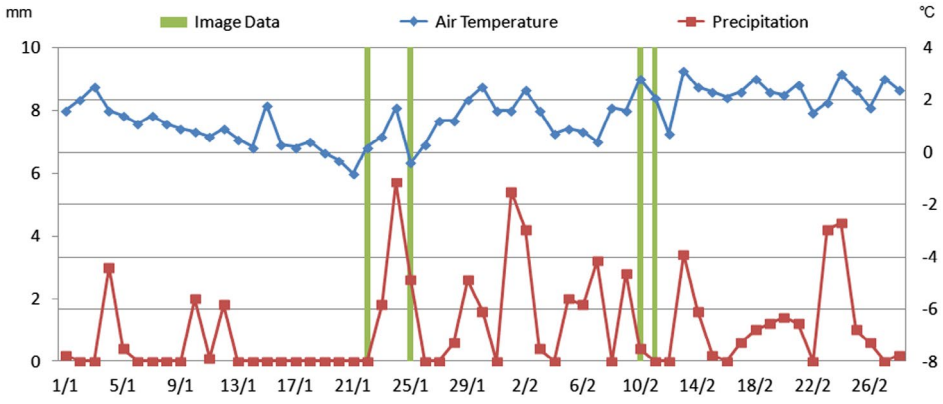


**Figure 5.** Temporal variations of mean daily air temperature and precipitation at site in January and February, 2011.



the uppermost centimetres. Several areas presented different rates of melting due to increases in the liquid water content in the snowpack in the Kraków Ice Field, and as a result, there were areas with lower backscattering signal (Figure 3). Thus, we distinguished two radar zones in the wet snow areas: the classical wet snow radar zone and another category with more melting water, named in this study as the slush snow radar zone. These categories belong to the same classical wet snow zone presented by Rau et al. (2000), but they were classified just to discriminate two snow zones with different amounts of liquid water, in order to analyse their spatio-temporal variability in the Kraków Ice Field during the period analysed in this study.

The classified images indicated that the lowest areas of the ice field were slush and wet snow radar zones (Figure 4(A)). The North, Northwest and Northeastward areas had more solar radiation and were predominantly wet snow and soaked snow radar zones (Figures 3 and 4(C)).

The sequence of the positive surface air temperatures recorded in the meteorological data and by field observations was related to the wet snow and soaked snow cover identified in the classified images. Meteorological data indicated several days in a row with negative temperatures near the acquisition of the COSMO-SkyMed images of 22 January 2013 and 25 January 2013 (Figure 5). This situation could cause the refreezing of water in the snow pack, including the formation of numerous subsurface ice pipes and lenses caused by melt-freeze cycles that are characteristic of a percolation radar zone (Figure 3(B)). However, rainfall events (field observation in Figure 6) and the sequence of the positive air temperatures caused the most extensive soaked snow radar zones identified in the COSMO-SkyMed image of the February 11 date (Figure 3(D)).

Rainfall induces occasional run-off peaks. According to Benn and Evans (1998), the highest weather-related discharges tend to be associated with high rainfall during summer storms and run-off in the basin, therefore contribute to snow and ice melting. Relatively poor correlation between run-off and meteorological variables during some days probably reflects a more complex relationship between meteorological variations and meltwater generation during periods of high snow precipitation.

The GPR data survey, which were obtained in January and February 2011 field activities (during one image date acquisition), revealed supraglacial liquid water storage (Figure 6) and englacial water inclusions along profiles of the Wanda glacier areas, located in the Kraków glacier (Rosa, Fernandez et al., 2014).

The classified COSMO-SkyMed images provided information about the existence of the hydrological systems in the supraglacial area during the period of January–February. Liquid water can be stored in a number of ways: in surface snow, in crevasses and in surface pools. Snow constitutes a major portion of the glacierized area, which changes during a season (Fountain 1996). It is possible to correlate the excess melting and rainfall peaks with discharge peaks in the glaciers. The meltwater

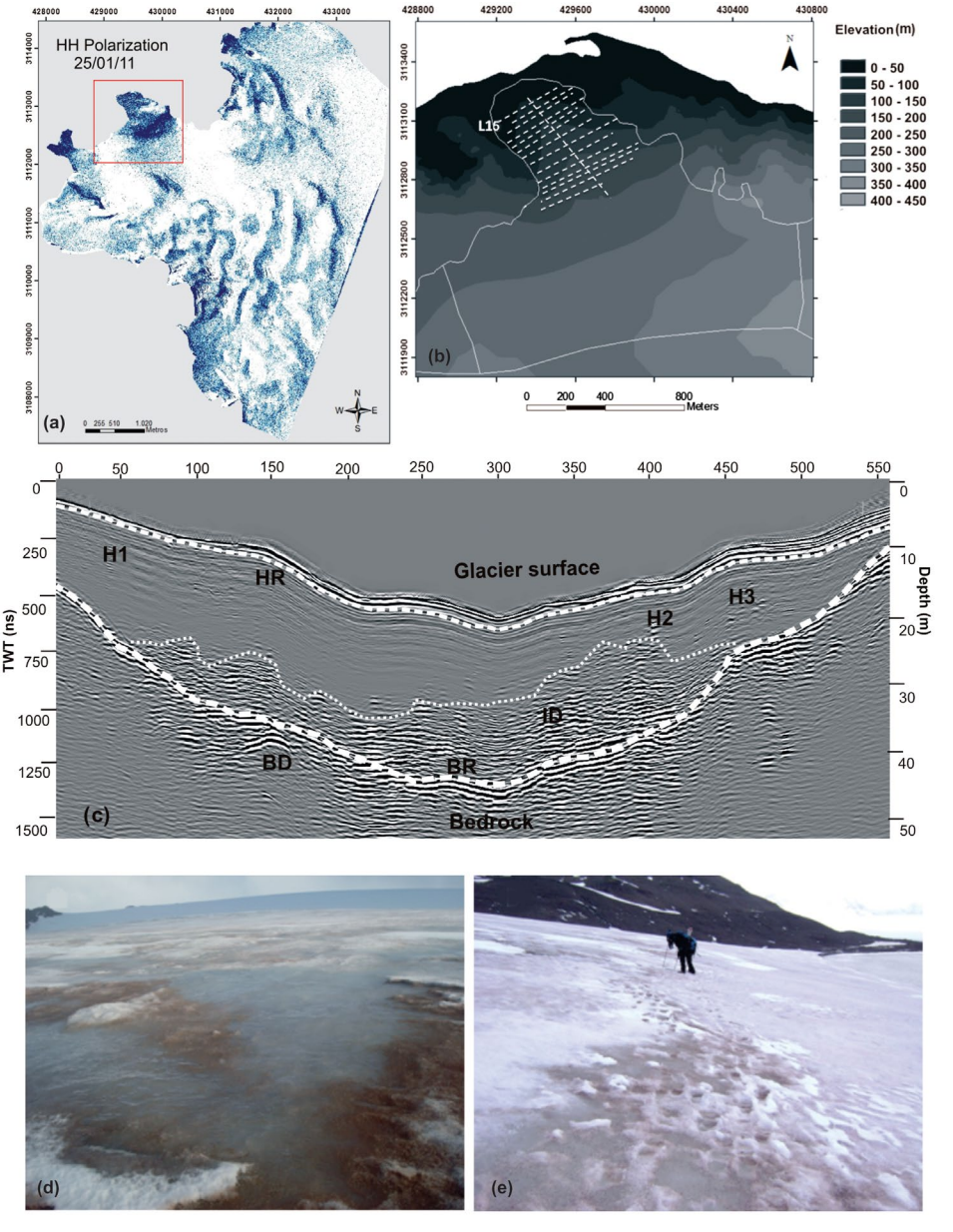


**Figure 6.** Supraglacial liquid water storage in the Wanda Glacier. (a) and (b) Location of the field observation and GPR acquisition in the end of January 2011. (c) Line L17 located in snout zone of the Wanda Glacier indicate supraglacial liquid water (slush) and wet snow (HR reflector). The classes HR, H, BR, ID and BD in GPR sections represent Horizontal Reflections, Diffraction Hyperbolae, Bed Reflections and Bed diffractions, respectively (Modified from Rosa, Fernandez et al., 2014). (d) and (e). Photographs of the L17 line GPR position are obtained in January 2011, during data image acquisition in the field campaigns show wet snow zone (e) sectors and (d) soaked snow areas.

produced in the wet snow zone, resulting in a loss of mass of the Kraków ice cap, can be potentially discharged to Admiralty Bay and the Bransfield Sea. The data obtained can be used to determine the melting patterns in the ablation season in the study area, and it can be used to analyse these phenomena in the other seasons.

## Conclusions

Surface snow cover is highly variable on the Kraków Ice Field. This variability was observed in field measurements as well as in the active microwave data. The surface snow, slush and percolation zones were identified on the Kraków Ice Field using a supervised classifier of minimum distance, considering the backscattering values of training samples in the COSMO-SkyMed imagery.

The percolation zone was more persistent in the highest parts of the Kraków Ice Field. Moreover, the highest areas of the Kraków Ice Field near Admiralty Bay exhibited more percolation zones than the areas near the Bransfield Strait. These results were consistent with previous studies performed by Vogt and Braun (2004), using ERS SAR images for the identification of radar zones in KGI glaciers during the 1998 ablation season.

The accuracy of DEM and COSMO-SkyMed data showed was satisfactory for snow radar zones determination in the analysed period. In comparison with other studies, as observed by Andrade et al. (2015) for Polar Club glacier (KGI), the high spatial and radiometric resolution, the VV polarized mode and incidence angle of the COSMO-SkyMed X-band images have high potential to discriminate snow cover.

The sensitivity of the radar signal to the snow-covered properties, such as the presence of liquid water, identified in this study, makes it a highly valuable tool to glacial melting dynamics analysis in remote areas, as demonstrated by Braun and Rau (2000) and Rau et al. (2000). Meteorological conditions prior to and during image acquisition have coherence of our mapped wet snow dynamics, classified in the COSMO-SkyMed images. The snow cover in the study area changes on a time scale of days to weeks, as observed by Rau et al. (2001) and Andrade et al. (2015).

Multitemporal COSMO-SkyMed snow-covered products and other SAR products provide the possibility of observing the glacier surface zones with high temporal and spatial resolutions at different polarizations. This methodology allows to monitor the snowmelt in study area and other glacial environments.



## Acknowledgement

The images used in this study were kindly provided under COSMO-SkyMed, Project 2294 from the Italian Space Agency (ASI).

## Disclosure statement

No potential conflict of interest was reported by the authors.

## Funding

This work was supported by the Brazilian National Council for Scientific and Technological Development (CNPq) [grant number 475478/2013-4] and FAPERGS.

## References

Andrade AM, Arigony-Neto J, Bremer LF, Michel RFM, Fassoni-Andrade AC, Schaefer CEGR, Simões JC. 2015. Cosmo-SkyMed X-band SAR data for classification of ice-free areas and glacier facies on Potter Peninsula, King George Island Antarctica. Geocarto Int. 30:1–10.

Arigony-Neto J. 2006. Monitoring glacier parameters on the Antarctic Peninsula – a centerline approach combining satellite and GIS data [PhD Thesis]. Freiburg: Universität Freiburg.

[ASI] Agenzia Spaziale Italiana. 2007. COSMO-SkyMed SAR products handbook. Roma: ASI Agenzia Spaziale Italiana.

Battazza F, CapuziA, Coletta A, Caltagirone F, Valentini G, Fagioli S, Angino G, Im-Pagnatiello F, Leonardi R. 2007. COSMO-SkyMed program: mission and system description of an advanced space EO dual-use asset. Proceedings of 27th EARSeL Symposium; 2007 Jun 4; Bolzano, Italy: EARSeL.

Benn DI, Evans DJA. 1998. Glaciers & Glaciation. London: Arnold; p. 734p.

Blindow N, Suckro SK, Rückamp M, Braun M, Schindler M, Breuer B, Saurer H, Simões JC, Lange MA. 2010. Geometry and thermal regime of the King George Island ice cap, Antarctica, from GPR and GPS. Ann Glaciol. 51:103–109.
Braun M, Gossmann H. 2002. Glacial changes in the area of Admiralty Bay and Potter Cove, King George Island, Antarctica. In: Beyer M, Boelter M, editors. Geoecology of terrestrial Antarctic Oases. Berlin: Springer Verlag; p. 75–89.
Braun M, Rau F. 2000. Using a multi-year data archive of ERS SAR imagery for the monitoring of firn line positions and ablation patterns on the King George Island ice cap (Antarctica). Proceedings of EARSeL-SIG-Workshop Land Ice and Snow; 2000 Jun 16-17; Dresden: EARSeL. Published on CD-Rom in 2001.
Bremer UF. 1998. Morfologia e bacias de drenagem da cobertura de gelo da ilha Rei George, Antártica. [Morphology and drainage basins of the King George Island ice cover, Antarctica] [dissertation]. Porto Alegre: Universidade Federal do Rio Grande do Sul. Portuguese.
Caltagirone F, Capuzi A, Leonardi R, Fagioli S, Angino G, Impagnatiello F. 2007. COSMO-SkyMed: an advanced dual use system for earth observation. Proceedings of IGARSS; 2007 Jul 23–27; Barcelona: IGARSS: p. 1–18.
[CCRS] Canada Centre for Remote Sensing. 2002. Remote Sensing in Canada (RSIC); p. 1-10.
Coletta A, Valentini G, Capuzi A, Caltagirone F, De Carlo M, De Luca G, Battazza F, Covello F. 2008. II programma COSMO-SkyMed. Riv Ital di Telerilev. 40:5–13.
Covello F, Battazza F, Coletta A, Lopinto E, Fiorentino C, Pietranera L, Valentini G, Zooli S. 2008. COSMO-SkyMed an existing opportunity for observing the earth. J Geodyn. Special Issue.
Cuffey K, Paterson WSB. 2010. The physics of glaciers. 4th ed. Amsterdam: Elsevier.
Ferrando FA, Vieira R, Rosa KK. 2009. Sobre el calentamiento global en la Isla Rey Jorge: procesos y evidencias en el glaciar Wanda y su entorno. [Global change in King George Island: processes and evidence in Wanda glacier and their next area]. Rev Inform Geog. 41: 25–40. Spanish.
Forster RR, Isacks BL, Das SB. 1996. Shuttle imaging radar (SIR-C/X-SAR) reveals near-surface properties of the South Patagonian Icefield. J Geophys Res. 101:169–169.
Fountain AG. 1996. Effect of snow and firn hydrology on the physical and chemical characteristics of glacial runoff. Hydrol Proc. 10:509–521.
Hall DK, Riggs GK, Salomonson VV. 1995. Development of methods for mapping global snow cover using moderate resolution imaging spectroradiometer data. Remote Sens Environ. 54:127–140.
Hall DK, Foster JL, Chien JYL, Riggs GA. 1995. Determination of actual snow-covered area using Landsat TM and digital elevation model data in Glacier National Park, Montana. Polar Rec. 31:191–198.
Hall DK, Riggs GA, Salomonson VV, DiGirolamo NE, Bayr KJ. 2002. Remote Sens Environ. 83:181–194.
Hall DK, Riggs GA, Foster JL, Kumar S. 2010. Development and validation of a cloud-gap filled MODIS daily snow-cover product. Remote Sens Environ. 114:496–503.
Hall DK, Crawford CJ, DiGirolamo NE, Riggs GA, Foster JL. 2015. Detection of earlier snowmelt in the Wind River Range, Wyoming, using Landsat imagery, 1972–2013. Remote Sens Environ. 162:45–54.
Jensen JR. 2007. Remote sensing of the environment: an earth resource perspective. 2nd ed. Upper Saddle River (NJ): Prentice Hall.
König M, Winther JG, Isaksson E. 2001. Measuring snow and glacier ice properties from satellite. Rev Geophys. 39:1–27.
Liu H, Wang L, Jezek K. 2005. Delineation of dry and melt snow zones in Antarctica using active and passive microwave observations from space. Geoscience and Remote Sensing Symposium; 2005 Jul 25–29; Seoul: IGARSS. 8, 5452–5455.
Macheret YY, Moskalevsky MY, Simões JC, Ladouch L. 1997. Radio echo-sounding of King George Island ice cap, South Shetland Islands, Antarctica. Mater Glyatsiol Issled Data Glaciol Stud. 83:121–128.
Mendes Jr. CW. 2011. Monitoramento da zona superficial de neve úmida da Península Antártica pelo uso de dados dos sensores SMMR e SSM/I [PhD Thesis]. Porto Alegre: Universidade Federal do Rio Grande do Sul.
Park BK, Chang SK, Yoon HI, Chung H. 1998. Recent retreat of ice cliffs, King George Island, South Shetland Islands, Antarctic Peninsula. Ann Glaciol. 27:633–635.
Partington KC. 1998. Discrimination of glacier facies using multi-temporal SAR data. J Glaciol. 44:42–53
Rao DP. 2002. International society for tropical ecology remote sensing application in geomorphology. Trop Ecol. 43:49–59
Rau F, Braun M, Saurer H, Gossmann H, Kothe G, Webei F, Ebel M, Beppler D. 2000. Monitoring multi-year snow cover dynamics on the Antarctic Peninsula using radar imagery. Polarforschung. 67:27–40.
Rau F, Braun M, Friedrich M, Weber F, Gossmann H. 2001. Radar glacier zones and their boundaries as indicators of glacier mass balance and climatic variability. EARSeL eProc. 1:317–327.
Rees WG, Satchell JF. 1997. The effect of median filtering on synthetic aperture radar images. Int J Remote Sens. 18:2887–2893.
Rosa KK, Mendes Jr. CW, Arigony-Neto J, Vieira R, Simões JC. 2013. Use of COSMO-SkyMed imagery for recognition of geomorphological features in the Martel Inlet ice-free areas, King George Island, Antarctica. Int J Remote Sens. 34:8936–8951.
Rosa KK, Fernandez GB, Rocha TB, Simões FL, Vieira R, Simões JC. 2014. Stratigraphy of Wanda Glacier, King George Island, Antarctica, using Ground Penetrating Radar. Rev Bras Geof. 32:21–30.

Rosa KK, Freiberger VL, Vieira R, Rosa CA, Simões JC. 2014. Glacial recent changes and climate variability in King George Island, Antarctica. Quat Environ Geosci. 5:176–183.
Rosa KK, Sartori R, Simões JC. 2015. Análise das mudanças ambientais da Geleira Viéville, Baía do Almirantado, Ilha Rei George, Antártica. [Environmental changes analysis of the Viéville Glacier, Admiralty Bay, King George Island, Antarctica]. Pesq Geoci. 42: 61–71. Portuguese.
Sarapirome S, Tassanasorn A, Suwanwerakamtorn R. 1995. Using Radar images as a tool to study geomorphology and geology of the Chaiyaphum area, Thailand. In: Wannakao L, editor. Proceedings of the International Conference on Geology, Geotechnology and Mineral Resources of Indochina; 1995 Nov 22–25; Thailand. Khon Kaen: Khon Kaen University.
Simões JC, Bremer UF. 1995. Investigations of King George Island ice cover using ERS-1/SAR and SPOT imagery. Rev SELPER. 11:56–60.
Simões JC, Ferron FA, Bernardo RT, Aristarain AJ, Stievenard M, Pouchet M, Delmas RJ. 2004. Ice core study from King George Island, South Shetlands, Antarctica. Pesq Ant Bra. 4:9–23.
Travassos JM, Simões JC. 2004. High-resolution radar mapping of internal layers of a subpolar ice cap, King George Island, Antarctica. Pesq Ant Bra. 4:57–65.
Vogt S, Braun M. 2004. Influence of glaciers and snow cover on terrestrial and marine ecosystems as revealed by remotely-sensed data. Pesq Ant Bras. 4:105–118.